Desalination and Water Treatment
www.deswater.com
doi: 10.1080/19443994.2013.787372

52 (2014) 365–374
January

Taylor & Francis
Taylor & Francis Group

Ammonia nitrogen removal from micro-polluted river by permeable reactive barriers: lab-scale study with steel slag and fly ash brick in combination as reactive media

Ruifang Qiu[a,b], Fangqin Cheng[a,*], Rui Gao[b], Jianfeng Li[a]

[a]*State Environmental Protection Key Laboratory of Efficient Utilization Technology of Coal Waste Resources, Institute of Resources and Environment Engineering, Shanxi University, # 92 Wucheng Road, Shanxi Province, Taiyuan 030006, China*
Tel. +86 13934551178; Fax: +86 351 7016893; email: cfangqin@sxu.edu.cn
[b]*College of Environmental & Resource Sciences, Shanxi University, Taiyuan 030006, China*

Received 17 October 2012; Accepted 4 March 2013

ABSTRACT

This paper focuses on the feasibility study of ammonia nitrogen removal from micro-polluted river by permeable reactive barriers with mixtures of steel slag and fly ash brick as reactive materials. The results indicated that individual maximum adsorption capacities of steel slag and fly ash brick were 0.83 and 0.42 mg/g, respectively. However, 3–5 mm steel slag was best for ammonia nitrogen removal in terms of removal efficiency and permeability. And the best ammonia nitrogen removal efficiency was 65.8% when the steel slag to fly ash brick ratio was 3:1. The study indicated that the steel slag and fly ash brick mixture is an effective reactive material in a permeable reactive barrier system to remove ammonia nitrogen from micro-polluted river.

Keywords: Steel slag; Fly ash brick; Ammonia nitrogen; Adsorption; Isotherms

1. Introduction

Permeable reactive barrier (PRB) has been used in many countries due to its low cost, continuity once installed, potential long duration, and effectiveness. When the contaminated plume goes through the barrier, the contaminants react with reactive materials to reduce the concentration based on adsorption, precipitation, and decomposition [1]. It has also been used for groundwater treatment to save operation and maintenance costs [2]. The reactive materials in permeable zone are crucial in PRB technology, which can be used separately or in combination depending on the types of contamination. Recent attempts have been made in PRBs to find the cost-effective reactive materials from industrial wastes, such as steel slag [3], fly ash [4], peat [5], and Fe^0 filings [6] etc. These materials are effective in removing particular contaminants and some are of great amount. If these industrial wastes can be used as reactive media in PRBs, it would save great land space and disposal costs. However, it should be noted that little has been known about using mixtures of steel slag and fly ash brick as reactive media. Steel slag, a main by-product in steelmaking process, consists of calcium oxide, magnesium oxide, and other metal oxides [3]. It has been used as an alternative adsorbent for dye [7], phosphorus [8],

*Corresponding author.

nickel [9], and arsenic [10], which would also be suitable for nitrogen removal. However, steel slag aggregates easily in water solution or moisture conditions, which would change the hydraulic conductivities and reduce the porosity gradually and finally in concomitance with clogging [11].

Fly ash brick is made of fly ash (above 75%) blended with appropriate lime and gypsum by steam curing. Fly ash brick has larger hydraulic conductivity, which makes it more permeable than steel slag. The elements presented in fly ash brick include silicone (Si), aluminum (Al), calcium (Ca), iron (Fe), magnesium (Mg), potassium (K), and sodium (Na). Some researchers have also reported that modified fly ash is effective for ammonia nitrogen removal [12]. It seems logical that using steel slag and fly ash brick in combination could not only exert higher NH_4^+-N removal efficiency of fly ash brick, but also prevent clogging due to its complex porous structure. Therefore, fly ash brick and steel slag in combination as PRB's reactive material was proposed in this study.

The objective of this work was to investigate the feasibility of using mixtures of steel slag and fly ash brick as PRB's material for the NH_4^+-N removal. Batch studies were conducted to investigate the impact of initial NH_4^+-N concentration, contact time, solution pH, particle size of steel slag on NH_4^+-N removal rate. The maximum NH_4^+-N adsorption capacity and isotherm were also analyzed. Furthermore, column tests with continuous flow were carried out to find the optimal volume ratio of steel slag to fly ash brick.

2. Materials and methods

2.1. Materials

Steel slag was supplied by Taiyuan iron and steel (group) Co. Ltd., China. It was crushed in a ball mill to mm-sized, then screened to different particle size ranges and washed with distilled water to remove surface dust and soluble ions. Fly ash brick was obtained from a brick factory in Taiyuan, China. It was made of coal fly ash (above 75%) blended with quicklime and gypsum under steam curing. The characteristics and composition of two materials are presented in Table 1. The NH_4^+-N solution for the experiments was prepared by NH_4Cl with distilled water.

2.2. Batch NH_4^+-N adsorption experiments

The adsorption capacity with contact time and the effect of initial NH_4^+-N concentrations were investigated in a series of 250 mL glass Erlenmeyer flask containing 5.0 g prepared steel slag (fly ash brick of crushed) with 100 mL NH_4^+-N solution. The concentration of NH_4^+-N was 5, 10, 25, 50, and 100 mg/L, respectively. All the glass Erlenmeyer flasks were continuously shaken for 6 h in a thermostat shaking container at 120 rpm to ensure equilibrium at 20˚C. This speed was fast enough to ensure constant mixing but not too fast to encourage disaggregation of particles [13]. The pH of all solutions was maintained at about 7.0 by adding NaOH (0.1 mol/L) or HCl (0.1 mol/L) solution. The particle size of steel slag was in the range 3–5 mm. Meanwhile, this batch equilibrium technique is used to investigate the capacity of adsorption [14]. The adsorption capacity of a combination of V_{slag}:$V_{fly\ ash}$ = 3:1 is conducted on the same condition.

The effect of adsorbent dosage on NH_4^+-N removal was tested by adding different adsorbent amounts into 100 mL of NH_4^+-N solution at 120 rpm on a rotary shake, respectively. The amount of steel slag (fly ash brick of crushed) with particle sizes of 3–5 mm are 1, 3, 5, 8, 10, and 13 g. The NH_4^+-N initial concentration is 10 mg/L and the solution pH was maintained at about 7.0 and 20˚C.

The effect of pH on NH_4^+-N removal was observed at NH_4^+-N initial concentration of 10 mg/L at various pH values (2, 4, 6, 7, 8, 10, and 13). About 5 g of steel slag (fly ash brick of crushed) was put in each glass of Erlenmeyer flasks which were shaken at 120 rpm and 20˚C. The particle size of adsorbents was between 3 and 5 mm. At different times, the adsorption capacity

Table 1
Characteristics and composition of steel slag and fly ash brick

Steel slag								
CaO	SiO_2	MgO	FeO	Al_2O_3	TFe	Cr_2O_3	TiO_2	MnO
51.84%	28.21%	9.74%	6.17%	4.39%	3.96%	1.28%	0.35%	0.29%
Coal fly ash brick								
SiO_2	Al_2O_3	Fe_2O_3	CaO	MgO	Na_2O	K_2O	SO_3	
50.6%	27.1%	7.1%	2.8%	1.2%	0.5%	0.3%	0.3%	

and the final pH were measured. In addition, 5 g combination of V_{slag}:$V_{fly\ ash}$ = 3:1 was put in 100 mL NH_4^+-N solution (initial pH is 7.0) under the same condition to investigate the change of pH value with reaction time.

The effect of particle size of steel slag was also investigated. The batch experiments were carried out using 5 g steel slag in 100 mL NH_4^+-N solution under above-mentioned conditions. The particle size of steel slag ranged from 3 mm to 24 mm (3–5 mm, 5–8 mm, 8–10 mm, 13–15 mm, 18–20 mm, and 23–25 mm).

The batch experiments for standard adsorption enthalpy ($\triangle H^0$) have been studied at 20, 30, and 40°C. A constant temperature batch was used to keep the temperature consistent. About 5 g of steel slag (fly ash brick of crushed, a combination of V_{slag}:$V_{fly\ ash}$ = 3:1) was added into a series of 100 mL NH_4^+-N solution of 10 mg/L under above-mentioned conditions.

2.3. Continuous-flow tests

The experimental setup is shown in Fig. 1. The reactor was made of acrylic in the dimension of 45 cm × 20 cm × 30 cm (L × H × W). About 5 cm quartz sand was added on the top and at the bottom of the box and supported by a macroporous board. Steel slag and fly ash brick were packed in the middle. The influent was pumped into the reactors continuously by a peristaltic pump at a rate of 150 mL/min. Three different volume ratios (steel slag to fly ash brick of crushed) were tested in this study, they are 1:1, 3:1, and 5:1 in Box 1#, 2#, and 3#, respectively. The system was operated for 14 days, and the effluent samples were collected daily for NH_4^+-N analysis.

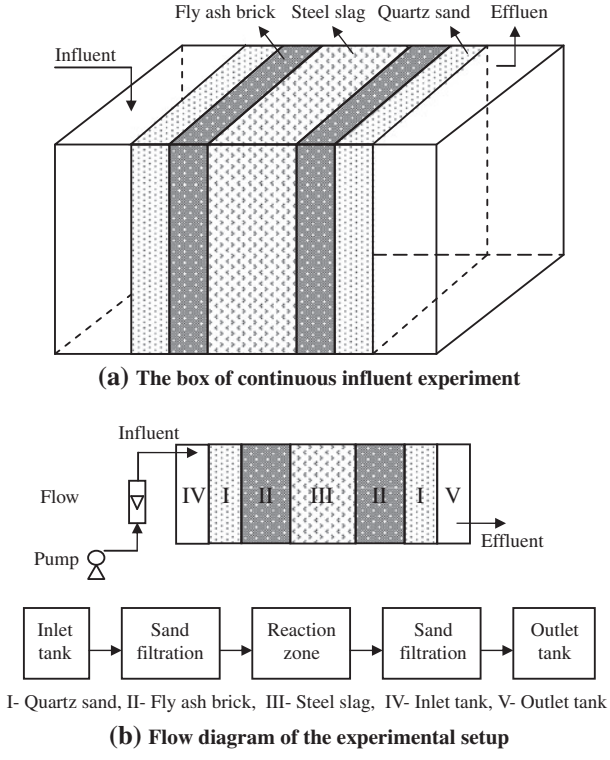

Fig. 1. Flow diagram of the experimental setup. The reactor was 45 cm × 20 cm × 30 cm (L × H × W); added 5 cm quartz sand on the top and at the bottom of the box; steel slag and fly ash brick were packed in the middle.

2.4. Analytical methods

Chemical compositions of the steel slag and coal fly ash brick were measured by X-ray-fluorescent (72000S, ARL, Switzerland). pH was measured using a pH meter (PHBJ-260, Leici, China). UV/visible spectrophotometer (UV-2,100, Shinco, China) was used to determine the concentrations of NH_4^+-N according to APHA methods [15]. All sorption experiments were conducted in triplicates and the data were expressed as the average value.

3. Results and discussion

3.1. Effect of initial NH_4^+-N concentration

The effect of initial NH_4^+-N concentration on NH_4^+-N removal by the two materials was investigated in this study, as shown in Fig. 2. It can be seen that the adsorption capacity of NH_4^+-N increased with the increase in contact time, but time for equilibrium varied when the initial NH_4^+-N concentration changes. Under the same condition, the time to establishe equilibrium for steel slag was longer than for fly ash brick. In every circumstance, NH_4^+-N uptake rate is higher at the start-up period. The initial rapid uptake rate may be due to the increase in available vacant sites, which increased the concentration gradient between adsorbates in the solution and adsorbates in the adsorbent [16]. And adsorption gradually decreased with reduced adsorption sites. The further increase in contact time had no obvious effect on the uptake rate after 60 min. It also can be noted that, NH_4^+-N removal was more efficient when the initial concentration is low. The effect of initial NH_4^+-N concentration on NH_4^+-N removal by fly ash brick was negligible when the initial concentration was lower than 50 mg/L (Fig. 2b). The experiment showed that the maximum adsorption capacities of steel slag and fly ash brick were 0.98 mg/g and 0.58 mg/g, respectively. Huo et al. [17] reported that NH_4^+-N removal reached 98.46% with an initial concentration of 6 mg/L by

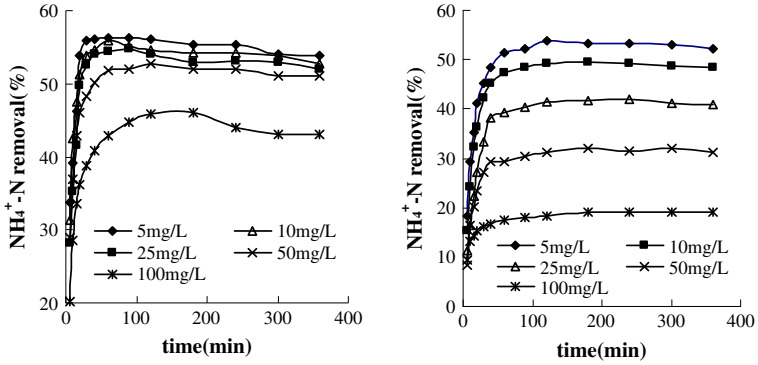

(a) Steel slag **(b)** Fly ash brick

Fig. 2. Effect of initial NH_4^+-N concentration on NH_4^+-N removal by two materials. Added 5 g steel slag (particle size: 3–5 mm) into 100 mL NH_4^+-N solution; changed NH_4^+-N concentration (5, 10, 25, 50, and 100 mg /L); shaken for 6 h at 120 rpm to ensure equilibrium at 20˚C; pH was controlled at 7.0 by dosing 0.1 mol/L NaOH/HCl. Fly ash brick of crushed was tested on the same condition.

modified clinoptilolite. But clinoptilolite needs modification by three steps used with NaCl solution and $FeCl_3$ solution of certain concentration and was calcinated at 200˚C in a muffle furnace for 1 h finally. Halim[18] et al. investigated the adsorption capacity of NH_4^+-N was 24.39 mg/g on the composite media of activated carbon and zeolite. Wang et al. [19] et al. found that the maximum theoretically saturated adsorption of NH^+_4–N was 2.33 mg/g for zeolite as filled materials in wetland system. Liu [20] et al. screen six novel agricultural residues as sorbents to treat NH_4^+-N, and the theoretical maximum adsorption capacities were 6.71, 4.62, 6.07, 5.01, 6.22, and 6.25 mg/g, respectively. Most studies on NH_4^+-N adsorption from aqueous solution have been focused on mineral materials and their modifications, which need large amounts of money and consume resources in large-scale application. Compared with other adsorbents from literature, steel slag and fly ash brick, as adsorbents not only solve problem of land occupation but also have a low-cost; their cost in environmental waste treatment would be an advantage.

3.2. Effect of adsorbent dosage

Fig. 3 shows that the uptake of the NH_4^+-N increased rapidly with increasing amount of adsorbent ranging from 1 to 5 g and slowed down to 10 g. A further increase in the amount of adsorbent did not affect the uptake significantly.

3.3. Effect of pH

The effect of pH on NH_4^+-N removal is shown in Fig. 4. Six pH values in range of 2–13 were tested. With the pH increased, the adsorption capacity of steel slag

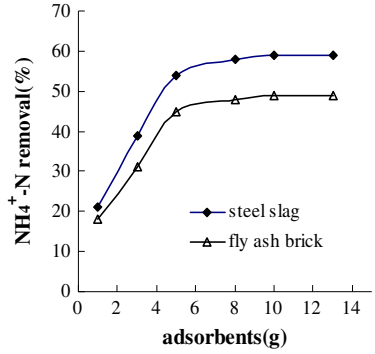

Fig. 3. Effect of adsorbent dosage on the removal of NH_4^+-N. Added Steel slag (particle size: 3–5 mm) into 100 mL NH_4^+-N solution (10 mg/L); changed the dosage (1, 3, 5, 8, 10 and 13 g); shaken for 6 h at 120 rpm at 20˚C; pH was controlled at 7.0 by dosing 0.1 mol/L NaOH/HCl. Fly ash brick of crushed was tested on the same condition.

increased slowly, but it was different for fly ash brick (Fig. 4a): The adsorption was found to decrease both at the lower and higher pH values with somewhat higher adsorption in the intermediate pH region. The pH in solution affects the adsorption process, which can be explained using the theory of zero point of charge (ZPC). The essential mineral of steel slag is magnetite whose ZPC is obtained at pH 6.5. When the pH < 6.5, the steel slag surface is protonated and became positively charged, which prevents electrostatic binding of the positively charged NH_4^+. In this case, the adsorption capacity is attributed to the porous of steel slag surface. But, for pH > 6.5, the surface becomes deprotonated, which favors the adsorption of NH_4^+ via electrostatic attraction [21]. For fly ash brick silica, alumina, and calcium compounds are the major constituents together with other metal oxides as minor or trace

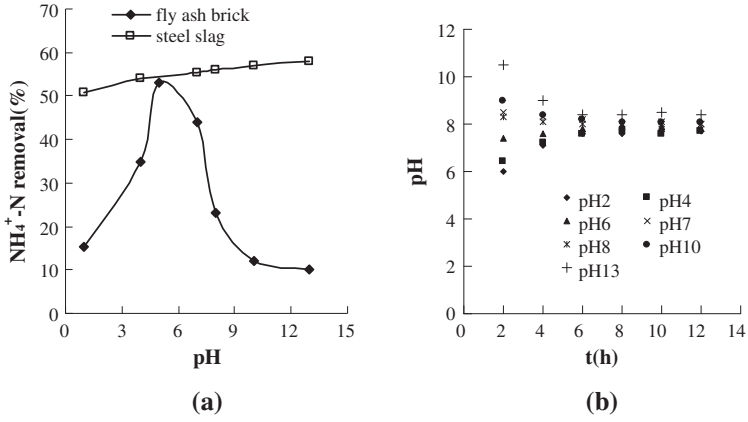

Fig. 4. Effect of solution pH on the removal of NH_4^+-N. Added 5 g steel slag (particle size: 3–5 mm) into 100 mL NH_4^+-N solution (10 mg/L); shaken at 120 rpm and 20°C; pH (2, 4, 6, 7, 8, 10, and 13) was controlled by dosing 0.1 mol/L NaOH/HCl. Fly ash brick of crushed (a combination of V_{slag}:$V_{fly\ ash}$ = 3:1) were tested on the same condition.

constituents, ZPC is 3.78 calculated theoretically [22], which adsorption capacity should increase with pH increasing. However, the adsorption behavior did not follow the theoretical predictions. Because the oxides of metals present in fly ash brick form aquo complexes and develop charged surface through amphoteric dissociation at varying pH values. At low pH (< 4), a positive charge is developed at the oxides surface in fly ash. Hence its uptake increased with the increasing of the solution pH at a lower pH value. In a higher pH range (>4), competitive cation Ca^{2+} had a much higher negative effect on ammonium removal. So its uptake decreased with the increasing of the solution pH at a higher pH value. The change of pH value with reaction time by a combination of V_{slag}:$V_{fly\ ash}$ = 3:1 is shown in Fig. 4(b). It was found that pH did not change dramatically and was close to the neutral levels with time elapsed, and then stabilized at 8 after 6 h.

3.4. Effect of particle size of steel slag

The effect of steel particle size on NH_4^+-N removal rate is shown in Fig. 5. When the particle size was less than 3–5 mm, the rise of NH_4^+-N uptake rate was not obvious. It is widely accepted that particle size would strongly influence on the adsorption. Smaller the steel slag particles, higher the specific surface area, which is directly related to NH_4^+-N removal efficiency. However, the clogging effect of small particles should be considered when selecting the appropriate steel slag size for NH_4^+-N removal, as smaller particles would have severe agglomeration.

3.5. Adsorption kinetics

In this study, batch adsorption kinetics of NH_4^+-N by steel slag and fly ash brick have been studied in terms of pseudo-first-order kinetic and pseudo-second-order kinetic model [23].

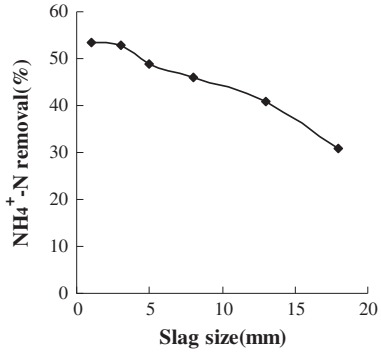

Fig. 5. Effect of particle size of steel slag on the removal of NH_4^+-N. Added 5 g steel slag (particle size: 3–5 mm) into 100 mL NH_4^+-N solution (10 mg/L); changed particle size (3–5 mm, 5–8 mm, 8–10 mm, 13–15 mm, 18–20 mm and 23–25 mm); shaken at 120 rpm and 20°C; pH was controlled at 7.0 by dosing 0.1 mol/L NaOH/HCl.

The integrating pseudo-first-order equation in the following:

$$\lg\left(\frac{Q_e}{Q_e - Q_t}\right) = \log Q_e - \frac{k_1}{2.303}t \quad (1)$$

where Q_e and Q_t are the amounts of solute adsorbed at equilibrium and at time t (min), respectively. And k_1 is the rate constant for pseudo-first-order reaction (min^{-1}). Eq. (1) can be rearranged to obtain a linear form:

$$\lg(Q_e - Q_t) = \log Q_e - \frac{k_1}{2.303}t \quad (2)$$

A straight line for the plot of lg (Q_e−Q_t) vs. t would suggest the applicability of this kinetic model fit the

Table 2
Parameters of kinetic models for NH_4^+-N adsorption by steel slag and fly ash brick

C_0 (mg/L)	Pseudo-first-order				Pseudo-second-order			
	Steel slag		Fly ash brick		Steel slag		Fly ash brick	
	k_1 (min^{-1})	R^2	k_1 (min^{-1})	R^2	k_2 [g/(mg min)]	R^2	k_2 [g/(mg min)]	R^2
5	0.024	0.8627	0.020	0.8165	1.01	0.9977	0.17	0.9994
10	0.021	0.8288	0.022	0.8543	0.69	0.9986	0.13	0.9988
25	0.018	0.7982	0.017	0.8872	0.23	0.9949	0.04	0.9978
50	0.016	0.8621	0.019	0.8959	0.21	0.9953	0.02	0.999
100	0.013	0.8026	0.013	0.8218	0.33	0.9940	0.01	0.9961

experimental data. The rate constant k_1 and correlation coefficients R^2, under different conditions were calculated from these plots as Table 2. We can see from Table 2 and Fig. 6, the R^2 values of the pseudo-first-order kinetic models were obviously lower.

The pseudo-second-order model can be expressed as Eq. (3), which can be rewritten as Eq. (4) in a linear equation form. And k_2 are the rate constant for pseudo-second-order reaction [g/(mg min)].

Pseudo-second-order equation:

$$\frac{d\mathrm{Q}}{d\mathrm{t}} = k_2(Q_\mathrm{e} - Q_\mathrm{t})^2 \tag{3}$$

Pseudo-second-order linear equation:

$$\frac{1}{Q_\mathrm{t}} = \frac{1}{k_2 Q_\mathrm{e}^2} \times \frac{1}{t} + \frac{1}{Q_\mathrm{e}} \tag{4}$$

A plot of $1/Q_\mathrm{t}$ vs. $1/t$ should give a linear relationship for the applicability of the pseudo-second-order kinetic. Table 2 and Fig. 7 show a plot of $1/Q_\mathrm{t}$ against $1/t$ for pseudo-second-order equation. Compared with R^2 values for the pseudo-first-order equation, the data show a good compliance with the pseudo-second-order equation and the regression coefficients R^2 for the linear plots are higher than 0.9940.

3.6. Adsorption capacity of NH_4^+-N by steel slag and fly ash brick combination

Adsorption equilibrium models have been widely applied to study the adsorption behavior, such as the Langmuir and Freundlich models. By applying these models, adsorption capacity can be obtained. In this study, the following equation for Langmuir model was used [24].

$$\frac{C_\mathrm{e}}{Q_\mathrm{e}} = \frac{1}{k_3 Q_\mathrm{m}} + \frac{C_\mathrm{e}}{Q_\mathrm{m}} \tag{5}$$

where Q_e and Q_m are the amounts of NH_4^+-N adsorbed per unit mass of adsorbent (mg/g) and the maximum adsorption capacity (mg/g), respectively;

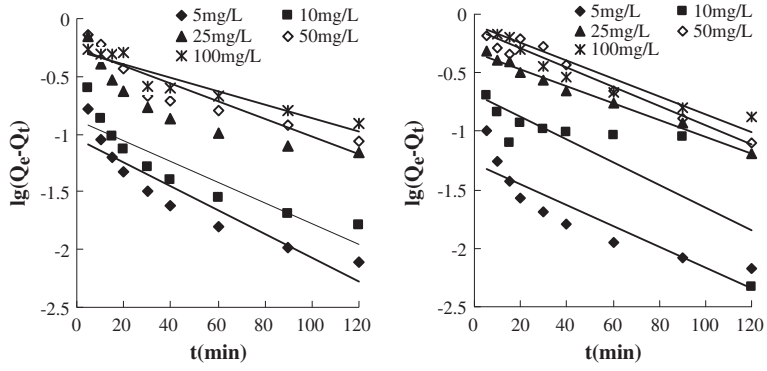

(a) Steel slag **(b)** Fly ash brick

Fig. 6. Pseudo-first-order kinetic of NH_4^+-N adsorption on steel slag and fly ash brick. Experimental condition is the same as the condition of Fig. 2.

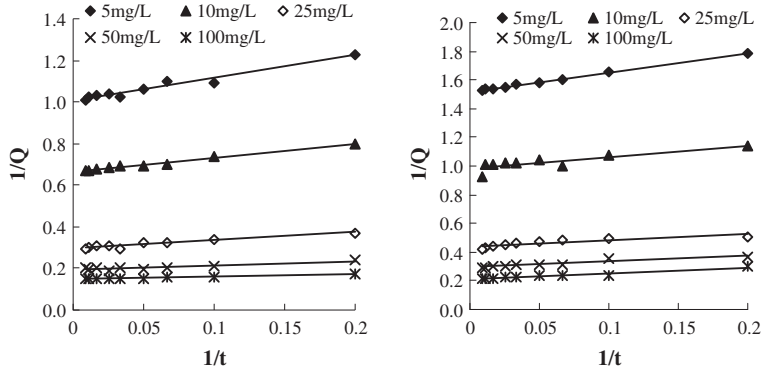

(a) Steel slag **(b)** Fly ash brick

Fig. 7. Pseudo-second-order kinetic of NH_4^+-N adsorption on steel slag and fly ash brick. Experimental condition is the same as the condition of Fig. 2.

C_e is the equilibrium NH_4^+-N concentration (mg/L) and k_3 is the Langmuir constant.

The essential characteristic of the Langmuir isotherm can be represented by the equilibrium parameter, R_L, calculated by:

$$R_L = \frac{1}{1 + k_3 C_0} \tag{6}$$

where C_0 is the initial NH_4^+-N concentration (mg/L). R_L is a dimensionless separation factor used to determine whether the adsorption process is favorable or unfavorable. The shapes of the isotherms for $0 < R_L < 1$, $R_L > 1$, $R_L = 1$, and $R_L = 0$ are favorable, unfavorable, linear, and irreversible [25], respectively.

Eq. (7) was used for the Freundlich model:

$$\ln Q_e = \frac{1}{n} \ln C_e + \ln k_f \tag{7}$$

where k_f and n are Freundlich adsorption isotherm constants, being indicative of the extent of the adsorption and the degree of nonlinearity between solution concentration and adsorption, respectively. The Freundlich constant n is a measure of the deviation from linearity of the adsorption. If a value for n is equal to unity the adsorption is linear. If a value for n is below unity, it implies that the adsorption process is chemical, but if a value for n is above unity, adsorption is a physical process [26].

Fig. 8 shows the Langmuir isotherm and Freundlich isotherm. The correlation coefficients (R^2) of Langmuir and Freundlich equations were 0.9969 ($p < 0.05$) and 0.9848 ($p < 0.05$) by steel slag, respectively, and 0.9819 ($p < 0.05$) and 0.9785 ($p < 0.05$) by fly ash brick, respectively. Furthermore, fitted equilibrium adsorption capacity ($Q_{\text{m-steel slag}} = 0.83\,\text{mg/g}$, $Q_{\text{m-fly ash brick}} = 0.42\,\text{mg/g}$) is in close agreement with those tested experimentally ($Q_{\text{m-steel slag}} = 0.98\,\text{mg/g}$, $Q_{\text{m-fly ash brick}} = 0.58\,\text{mg/g}$). Given the good agreement between model fit and experimentally tested equilibrium adsorption capacity in addition to the large correlation coefficients and higher significant level, it suggests that

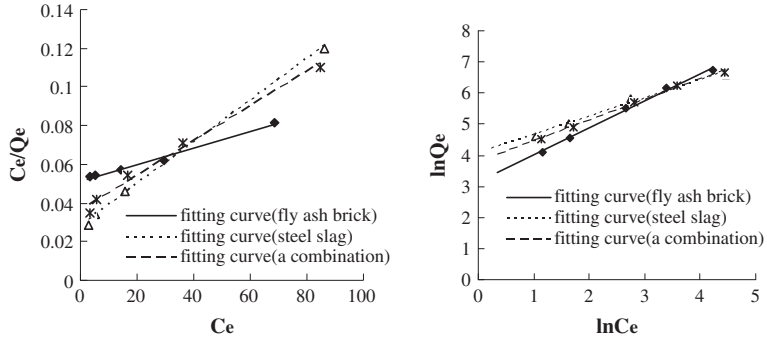

(a) Langmuir isotherm **(b)** Freundich isotherm

Fig. 8. The fitting curves with Langmuir and Freundlich equations. Experimental condition is the same as the condition of Fig. 2.

NH_4^+-N adsorption on two materials both followed their isotherms.

All the values of R_L calculated were found less than unity ($R_L = 0.004$–0.060 for steel slag, $R_L = 0.023$–0.081 for fly ash brick), and therefore the adsorption of NH_4^+-N is favorable. The Freundlich constant n of steel slag and fly ash brick at equilibrium (room temperature) are 1.69 and 1.42, respectively. The n values indicated that adsorption of these materials was favorable; and therefore this suggests it is more like a physical process, in which the adsorption bond becomes weak and conducted with van der Waals forces, rather than chemical process [27].

To determine if it was physical adsorption, standard adsorption enthalpy ($\triangle H^0$) was analyzed. The value of $\triangle H^0$ can be calculated from the van't Hoff plot equation (Eq. (8)) as follows.

$$\lg C_e = -\lg K_0 + \Delta H^0/(2.303RT) \quad (8)$$

where T is the absolute temperature (K), K_0 is constant and R is the gas constant. If $\triangle H^0 > 0$, the adsorption is endothermic. If $\triangle H^0 < 0$, the adsorption is exothermic. When attraction between adsorbates and an adsorbent took place, the change in standard enthalpy was caused by various forces, including van der Waals, hydrophobicity, hydrogen bonds, ligand exchange, dipole-dipole interactions, and chemical bonds [28]. According to the magnitude of different forces, the nature of physical or chemical adsorption can be identified by the sum of different forces. Generally, the magnitude of standard enthalpy changes for absolute physical adsorption is less than 20 kJ/mol, while chemical adsorption is in the range of 80–200 kJ/mol [29]. To obtain valuable knowledge about $\triangle H^0$, adsorption reaction was conducted at different temperatures (293, 303 and 313 K). The values of $\triangle H^0$ of steel slag adsorption and fly ash brick adsorption are 5.69, 5.38, 5.12 kJ/mol and 4.75, 4.53, 4.32 kJ/mol at 293, 303, and 313 K, respectively. The positive values of $\triangle H^0$ implied both the steel slag adsorption and fly ash brick adsorption are endothermic. In addition, both the adsorptions should be regarded as physical adsorption.

As the combination of $V_{\text{steel slag}}$: $V_{\text{fly ash brick}}$ was 3:1, the R^2 values (0.9969 ($p < 0.05$) and 0.9848 ($p < 0.05$) for Langmuir and Freundlich equations, respectively) showed that the adsorption process can be represented by two isotherms. The values of R_L are 0.035–0.078, less than unity, therefore the adsorption is favorable. The Freundlich constant n is 1.53 and the thermodynamic parameter $\triangle H^0$ are 5.44, 5.21, 4.83 kJ/mol at 293, 303 and 313 K, respectively, which presented the adsorption is endothermic and physical.

3.7. Removal of NH_4^+-N from continuous influent

Continuous flow tests were conducted for 14 days using experiment set up shown in Fig. 1. NH_4^+-N concentration in the influent was 10 mg/L. NH_4^+-N removal efficiency profile was shown in Fig. 9. The results showed that NH_4^+-N was reduced largely after the boxes. At the beginning, the NH_4^+-N removal increased dramatically that mainly due to the higher NH_4^+-N adsorption capacity, when the adsorbent mixture was fresh and the adsorption sites were free for NH_4^+-N. Then, the NH_4^+-N removal increased slowly after 6 days, which may be due to physical blockage of the adsorption sites. The average NH_4^+-N removal by box 1#, box 2#, and box 3# were 56.1, 65.8, and 60%, respectively. With the increasing amount of steel slag from box 1# to box 3#, NH_4^+-N removal efficiency of box 2# is higher than box 1# but did not continue trending higher of box 3#. It can be attributed to the fact that the porosity decreased obviously and clogging seriously with too high percentage composition of steel slag. With time going on, finally the difference of NH_4^+-N removal efficiency of three boxes was not evident (all the NH_4^+-N removal efficiency are about 60%). It may be due to the effect of biological nitrification. It is well known that biological nitrification is the most effective process for nitrogen removal [30]. The biological nitrification was in highest flight for NH_4^+-N removal in the columns as the time goes on. Therefore, the mixture of steel slag and fly ash brick was feasible for NH_4^+-N removal, and a proper volume ratio of steel slag and fly ash brick can improve the effluent quality.

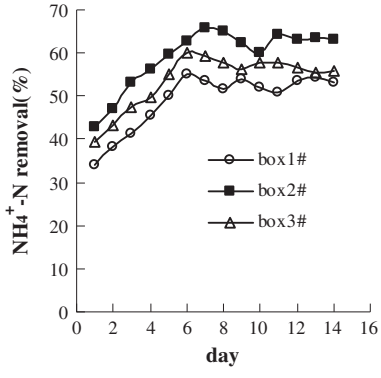

Fig. 9. NH_4^+-N removal from effluent through steel slag and fly ash brick boxes. The influent entered into reactor by a peristaltic pump at 150 mL/min; volume ratios of filler changed ($V_{\text{steel slag: fly ash brick of crushed}}$=1:1, 3:1 and 5:1); the system was operated for 14 days.

4. Conclusions

Present study indicates that steel slag and fly ash brick may be effective materials for NH_4^+-N removal in PRB systems. All NH_4^+-N adsorption behavior, respectively by steel slag, fly ash brick and combination of steel slag and fly ash brick, followed Langmiur and Freundlich models, and were preferential types and physical adsorption by isotherm and thermodynamics parameter analysis. Furthermore, the adsorption process was well described by the pseudo-second-order equation. The maximum adsorptions of steel slag and fly ash brick were 0.83 and 0.42 mg/g, respectively. The NH_4^+-N removal by steel slag decreased with increasing NH_4^+-N concentration, particle size, and solution pH. But NH_4^+-N removal by fly ash brick decreased with increasing NH_4^+-N concentration and it was at its peak at about pH 4. Continuous flow test showed the average rates of NH_4^+-N removal were around 56.1–60% by box $1^{\#}$, box $2^{\#}$, and box $3^{\#}$. The proper volume ratio of the mixture is 3:1 of steel slag to fly ash brick. Due to low cost and high adsorptive capacity, the mixture of steel slag and fly ash brick was the potential materials for NH_4^+-N removal from micro-polluted rivers.

The more long-term performance flow-through experiments should be explored further, which are important in the study of the contributions of denitrification by microbes. It may attain better NH_4^+-N removal efficiency.

Acknowledgments

This study was financially supported by the International cooperation program (No. 2011DFA 90830) from the Chinese Ministry of Science and Technology and Water Resources Department of Shanxi Province.

References

[1] EPA, Field applications of in situ remediation technologies: permeable reactive barriers, National Service Center for Environmental Publications (NSCEP), Cincinnati, OH, 2002.
[2] M.A. Carey, B.A. Fretwell, N.G. Mosley and J.W.N. Smith, Guidance on the Use of Permeable Reactive Barriers for Remediating Contaminated Groundwater, National Groundwater and Contaminated Land Centre Report NOC/01/51, Environment Agency, Entec (UK) Ltd, Solihull, 2002.
[3] V.K. Jha, Y. Kameshima, A. Nakajima, K. Okada, Hazardous ions uptake behavior of thermally activated steel–making slag, J. Hazard. Mater. 114 (2004) 139–144.
[4] B. Prasad, K. Sangeeta, B.K. Tewary, Fly ash zeolite as permeable reactive barrier for prevention of groundwater contamination due to coal ash disposal, Asian J. Chem. 24 (2012) 1045–1050.
[5] C.M. Su, R.W. Puls, Removal of added nitrate in cotton burr compost, mulch compost, and peat: Mechanisms and potential use for groundwater nitrate remediation, Chemosphere 66 (2007) 91–98.
[6] S.W. Jeen, R.W. Gillham, A. Przepiora, Predictions of long-term performance of granular iron permeable reactive barriers: Field-scale evaluation, J. Contam. Hydrol. 123 (2011) 50–64.
[7] Y.J. Xue, H.B. Hou, S.J. Zhu, Adsorption removal of reactive dyes from aqueous solution by modified basic oxygen furnace slag: Isotherm and kinetic study, Chem. Eng. J. 147 (2009) 272–279.
[8] C.G. Lee, J.A. Park, S.B. Kim, Phosphate removal from aqueous solutions using slag microspheres, Desalin. Water Treat. 44 (2012) 229–236.
[9] N. Ortiz, M.A. Pires, J.C. Bressiani, Use of steel converter slag as nickel adsorber to wastewater treatment, Waste Manage. 2 (2001) 631–635.
[10] C.S. Jeon, T. Batjargal, C.I. Seo, Removal of As (V) from aqueous system using steel making by-product, Desalin. Water Treat. 7 (2009) 152–159.
[11] J. Yang, S. Wang, Z.B. Lu, J. Yang, S.J. Lou, Converter slag-coal cinder boxs for the removal of phosphorous and other pollutants, J. Hazard. Mater. 168 (2009) 331–337.
[12] K. Xu, T. Deng, J.T. Liu, Study on the phosphate removal from aqueous solution using modified fly ash, Fuel 89 (2010) 3668–3674.
[13] B. Kostura, H. Kulveitova, J. Lesko, Blast furnace slag as sorbents of phosphate from water solutions, Water Res. 39 (2005) 1795–1802.
[14] B. Armagan, O. Ozdemir, M. Turan, Adsorption of negatively charged azo dyes onto surfactant-modified sepiolite, J. Environ. Eng. 129 (2003) 709–715.
[15] APHA, Standards Methods for the Examination of Water and Wastewater, Twentieth ed., American Public Health Association, Washington, DC, USA, 1998.
[16] M.S. Chiou, H.Y. Li, Adsorption behavior of reactive dye in aqueous solution on chemical cross-linked chitosan beads, Chemosphere 50 (2003) 1095–1105.
[17] H.X. Huo, H.L. Lin, Y.B. Dong, H.C. Han, Ammonia-nitrogen and phosphates sorption from simulated reclaimed waters by modified clinoptilolite, J. Hazard. Mater. 230 (2012) 292–297.
[18] A. Halim, H. Abdul Aziz, M.A. Megat Johari, K.S. Ariffin, Comparison study of ammonia and COD adsorption on zeolite, activated carbon and composite materials in landfill leachate treatment, Desalination 262 (2010) 31–35.
[19] Y.Q. Wang, S.J. Liu, Z. Xu, T.W. Han, Ammonia removal from leachate solution using natural Chinese clinoptilolite, J. Hazard. Mater. 136 (2006) 735–740.
[20] H.W. Liu, Y.H. Dong, Y. Liu, H.Y. Wang, Screening of novel low-cost adsorbents from agricultural residues to remove ammonia nitrogen from aqueous solution, J. Hazard. Mater. 178 (2010) 1132–1136.
[21] A.M. Carmo, L.S Hundal, M.L Thompson, Sorption of hydrophobic organ in compounds by soil materials: Application of unit equivalent freundlich coeficients, Environ. Sci. Technol. 34 (2000) 4363–4369.
[22] M. Sarkar, P.K. Acharya, Use of fly ash for the removal of phenol and its analogues from contaminated water, Waste Manage. 26 (2006) 559–570.
[23] S.B. Wang, E. Ariyanto, Competitive adsorption of malachite green and Pb ions on natural zeolite, J. Colloid Interface Sci. 314 (2007) 25–31.
[24] A.O. Alade, O.S. Amuda, A.O. Ibrahim, Isothermal studies of adsorption of acenaphthene from aqueous solution onto activated carbon produced from rice (Oryza sativa) husk, Desalin. Water Treat. 46 (2012) 87–95.
[25] K.R. Hall, L.C. Eagleton, A. Acrivos, T. vermeulen, Pore and solid diffusion Kinetics in fixed bed adsorption under constant pattern conditions, Ind. Eng. Chem. Fundam. 5 (1966) 212–223.
[26] Y.S. Li, P. Robin, D. Cluzeau, Vermifiltration as a stage in reuse of swine wastewater: Monitoring methodology on an experimental farm, Ecol. Eng. 32 (2008) 301–309.

[27] O. Adnan, O. Cigdem, E. Yunus, Modification of bentonite with a cationic surfactant: An adsorption study of textile dye Reactive Blue 19, J. Hazard. Mater. 140 (2007) 173–179.
[28] B. von Oepen, W. Kordel, W. Klein, Sorption of nonpolar and polar compounds to soils: Processes, measurements and experience with the applicability of the modified OECD-Guideline 106, Chemosphere 22 (1991) 285–304.
[29] B. Gu, J. Schmitt, Z. Chen, L. Liang, J.F. McCarthy, Adsorption and desorption of natural organic matter on iron oxide: mechanisms and models, Environ. Sci. Technol. 28 (1994) 38–46.
[30] D.S. Sun, X.D. Zhang, Y.D. Wu, Adsorption of anionic dyes from aqueous solution on fly ash, J. Hazard. Mater. 18 (2010) 335–342.